# Elastic and viscoelastic behavior of a magnetic recording tape

by B. S. Berry W. C. Pritchet

The mechanical behavior of a trilayer Mylarbased magnetic recording tape has been studied by three complementary methods, applied either to the complete tape or to samples prepared by the selective removal of its front or back coatings. One method provided tensile stress-strain and creep data, another exploited the phenomenon of thermal curling, and a third or mandrel method was used to measure relaxation and recovery in simple bending. Despite the large relative thickness of the Mylar substrate, both the initial stiffness and subsequent relaxation behavior of the tape were strongly influenced by the surface magnetic coatings, and particularly by the oriented and calendered frontcoat, which exhibited elastic anisotropy and an enhanced longitudinal Young's modulus of up to five times that of the Mylar core. As a consequence, the magnetically active frontcoat emerged as the most highly stressed component of the tape, and initially supported almost half of an imposed tensile load. The high initial modulus of the oriented and calendered frontcoat was attributed to the

©Copyright 1988 by International Business Machines Corporation. Copying in printed form for private use is permitted without payment of royalty provided that (1) each reproduction is done without alteration and (2) the *Journal* reference and IBM copyright notice are included on the first page. The title and abstract, but no other portions, of this paper may be copied or distributed royalty free without further permission by computer-based and other information-service systems. Permission to *republish* any other portion of this paper must be obtained from the Editor.

reinforcement provided by the magnetic oxide dispersed in the polymeric frontcoat binder. The substantial viscoelastic behavior of the coatings was also linked to their composite structure, and specifically to the ability of the binder to relax the enhanced initial modulus conferred by the presence of the oxide.

# 1. Introduction

Magnetic recording tapes of the type used for audio, video, or data storage are fabricated by the application of one or more thin surface coatings to a polymeric supporting substrate such as Mylar.\* From the viewpoint of mechanical behavior, such a multilayer represents a composite viscoelastic system, and exhibits creep and stress-relaxation which can influence the service performance of the tape. This study was concerned with the mechanical behavior of a trilayer tape which consisted of a substrate of 0.92-mil-thick Mylar, a 0.16-mil-thick frontcoat of magnetic CrO<sub>2</sub> particles in a polymeric binder, and a backcoat of nominally similar composition and thickness. The frontcoat used for data storage was easily distinguished from the backcoat, since the frontcoat received a calendering (warm-rolling) treatment that produced a high-gloss surface finish. To characterize the behavior of the tape, three simple but innovative mechanical tests were applied both to the complete tape and to samples from which one or both of the surface coatings had been removed. Tensile stress-strain and isoload creep

<sup>•</sup>Mylar is a biaxially oriented film of poly(ethylene terephthalate) produced by E. I. du Pont de Nemours and Co., Inc., Wilmington, DE.

# Elastic and viscoelastic behavior of a magnetic recording tape

by B. S. Berry W. C. Pritchet

The mechanical behavior of a trilayer Mylarbased magnetic recording tape has been studied by three complementary methods, applied either to the complete tape or to samples prepared by the selective removal of its front or back coatings. One method provided tensile stress-strain and creep data, another exploited the phenomenon of thermal curling, and a third or mandrel method was used to measure relaxation and recovery in simple bending. Despite the large relative thickness of the Mylar substrate, both the initial stiffness and subsequent relaxation behavior of the tape were strongly influenced by the surface magnetic coatings, and particularly by the oriented and calendered frontcoat, which exhibited elastic anisotropy and an enhanced longitudinal Young's modulus of up to five times that of the Mylar core. As a consequence, the magnetically active frontcoat emerged as the most highly stressed component of the tape, and initially supported almost half of an imposed tensile load. The high initial modulus of the oriented and calendered frontcoat was attributed to the

©Copyright 1988 by International Business Machines Corporation. Copying in printed form for private use is permitted without payment of royalty provided that (1) each reproduction is done without alteration and (2) the *Journal* reference and IBM copyright notice are included on the first page. The title and abstract, but no other portions, of this paper may be copied or distributed royalty free without further permission by computer-based and other information-service systems. Permission to *republish* any other portion of this paper must be obtained from the Editor.

reinforcement provided by the magnetic oxide dispersed in the polymeric frontcoat binder. The substantial viscoelastic behavior of the coatings was also linked to their composite structure, and specifically to the ability of the binder to relax the enhanced initial modulus conferred by the presence of the oxide.

# 1. Introduction

Magnetic recording tapes of the type used for audio, video, or data storage are fabricated by the application of one or more thin surface coatings to a polymeric supporting substrate such as Mylar.\* From the viewpoint of mechanical behavior, such a multilayer represents a composite viscoelastic system, and exhibits creep and stress-relaxation which can influence the service performance of the tape. This study was concerned with the mechanical behavior of a trilayer tape which consisted of a substrate of 0.92-mil-thick Mylar, a 0.16-mil-thick frontcoat of magnetic CrO<sub>2</sub> particles in a polymeric binder, and a backcoat of nominally similar composition and thickness. The frontcoat used for data storage was easily distinguished from the backcoat, since the frontcoat received a calendering (warm-rolling) treatment that produced a high-gloss surface finish. To characterize the behavior of the tape, three simple but innovative mechanical tests were applied both to the complete tape and to samples from which one or both of the surface coatings had been removed. Tensile stress-strain and isoload creep

<sup>•</sup>Mylar is a biaxially oriented film of poly(ethylene terephthalate) produced by E. I. du Pont de Nemours and Co., Inc., Wilmington, DE.

measurements are covered in Sections 2 and 3, the use of thermal curling measurements is introduced in Section 4, and a convenient mandrel method for relaxation and recovery measurements in simple bending is described in Section 5. As we shall see, and contrary perhaps to initial expectation, the results obtained clearly demonstrate the important role of the frontcoat in both the elastic and viscoelastic behavior of the tape.

# 2. Initial elastic moduli of the component layers

#### • Testing and stripping procedures

The basic approach followed in the tension tests was to make use of a relatively long sample, so that small strains produced easily measurable elongations. The apparatus shown in Figure 1 was an arrangement for the application of weights to a piece of tape about a meter long. To steady the tape and prevent torsional oscillation, the tape was tilted a few degrees off-vertical and passed over a 3/16-inch steel roller mounted in ball bearings. The microscope used for the elongation measurements was fitted with a 0.150-inch eyepiece scale graduated in 10<sup>-3</sup> inches per division, and was focused on the tape just above the steadying roller. It was found unnecessary to apply a fiducial mark to the tape, since a convenient bright spot could always be picked out from the illuminated field of view. For the modulus measurements, the principal concern was to apply the load for the shortest possible time, so that the "initial modulus" obtained experimentally approached the ideal unrelaxed modulus as closely as possible. With some practice and the use of two operators working together, each elongation measurement could be made in roughly 5 s. After each reading, the load was removed to check for the absence of creep. The overall loading pattern therefore had the form shown in Figure 1, and the initial moduli obtained experimentally may be thought of as "5-second moduli."

The procedure adopted to obtain the initial moduli of the component layers was to test the same sample before and after selective removal of the coatings with the solvent tetrahydrafuran. Selective stripping of just one coating was achieved by first placing the tape on a flat metal plate and slightly overlapping its edges with Scotch tape to protect the underside from the solvent. The exposed top coating was then removed by swabbing with the solvent. After the tape had been allowed to dry for an hour, a straight steel strip 3/8 inches wide was lightly clamped over the tape to act as a cutting guide for a scalpel. In this way a single-sided tape 3/8 inches wide was obtained from the original 1/2-inch-wide double-sided tape. Removal of the final layer could of course be accomplished without further trimming of the tape. After each of these steps, the mean thickness of the tape was determined from measurements at many individual points using a Starrett dial gauge with a 4-inch dial and a reading resolution of 20 microinches.

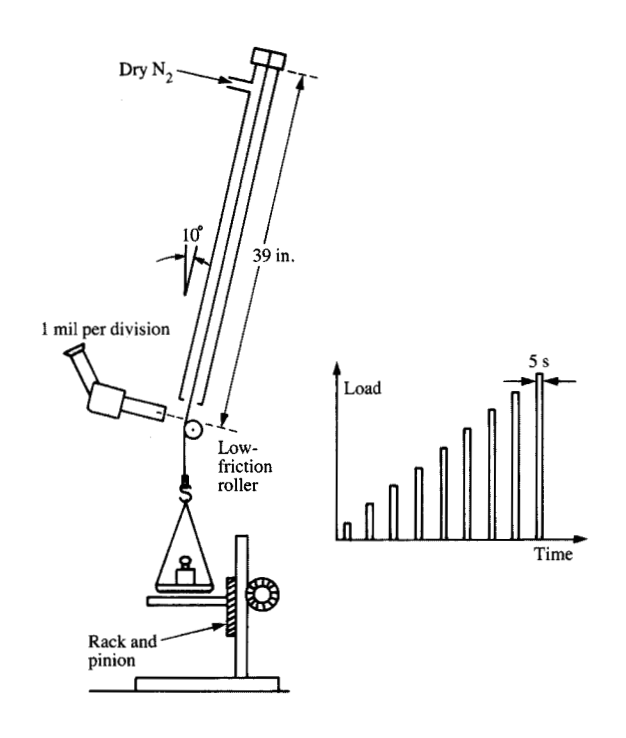


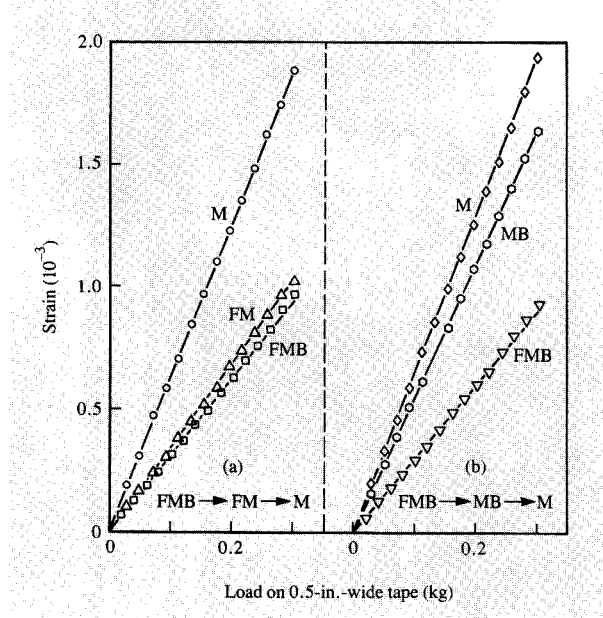
#### Figure i

The arrangement for elasticity and creep measurements under a tensile load. Also illustrated is the loading sequence used for the determination of the "5-second" modulus.

#### Results

The stripping procedures described above can be used to decompose the trilayer tape FMB (Frontcoat-Mylar-Backcoat) in the sequence  $FMB \rightarrow FM \rightarrow M$  or  $FMB \rightarrow MB \rightarrow M$ . The comparison obtained using both of these sequences turned out to be highly significant, and is shown in Figures 2 and 3 in the form of load-strain and stress-strain curves, respectively. To facilitate comparison, all of the data of Figure 2 have been scaled to load per 0.5inch width, so as to factor out the width reduction to 0.375 inches associated with the stripping process. Highly linear plots were observed in all cases up to loads of 0.23 kg (0.5 lb). Above that level, a slight upward deviation in the FMB data (only) marks the onset of detectable creep within the 5-s loading interval. A point of major significance is the distinct difference in the slopes of the FM and MB lines, which provided a direct proof that the frontcoat was substantially stiffer than the backcoat.

To proceed with analysis of the data, we introduce a parameter S to denote the inverse slope of the load-strain



#### Emma 2

Load-strain curves at 295 K for samples of trilayer tape, stripped in the sequence (a)  $FMB \rightarrow FM \rightarrow M$  and (b)  $FMB \rightarrow MB \rightarrow M$ . The marked difference in the slope of the lines FM and MB reveals the elastic asymmetry of the trilayer.

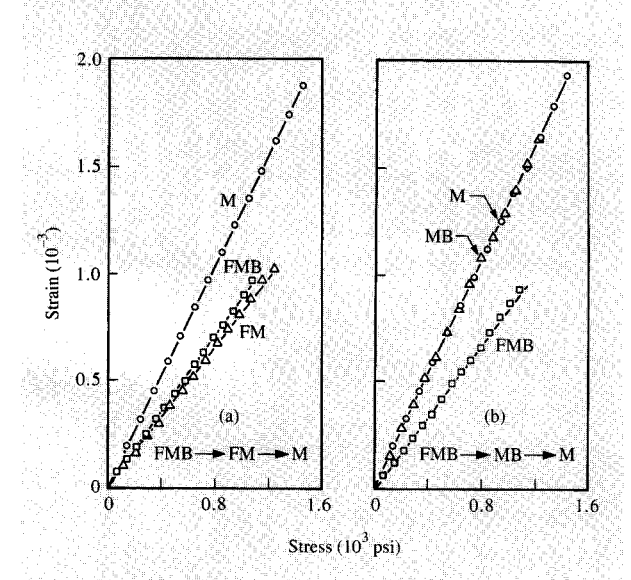


## Figure 3

The data of Figure 2 replotted in the form of stress-strain curves whose inverse slopes provide the moduli  $E_{\rm M},\,E_{\rm FM},\,E_{\rm MB},\,{\rm and}\,E_{\rm FMB}$  discussed in the text and listed in Table 1.

 Table 1
 Composite and component Young's moduli of trilayer tape.

$E_{ extsf{FMB}}$	$E_{\rm FM}$	$E_{\mathrm{MB}}$	$E_{\mathrm{M}}$	$E_{\mathtt{B}}$	$E_{ m F}$		
	(10 <sup>5</sup> psi)						
11.4	12.2	7.5	7.7	6.5	38.9		
		11.4 12.2	(10 <sup>5</sup> p	(10 <sup>5</sup> psi)	(10 <sup>5</sup> psi)  11.4 12.2 — 7.7 6.5	(10 <sup>5</sup> psi)  11.4 12.2 — 7.7 6.5 38.9	

<sup>\*</sup> As shown in Figures 1 and 2.

plots. The quantity S has the general significance of a tensile stiffness constant, and may be written as

$$S \equiv (L/\varepsilon) = EA,\tag{1}$$

where L denotes the applied load, e is the corresponding strain, A is the cross-sectional area, and E is the initial or 5-second modulus which represents our closest approach to the unrelaxed modulus  $E^U$ . For each of the cases shown in Figure 2(a), Equation (1) becomes

$$S_{\mathsf{M}} = E_{\mathsf{M}} A_{\mathsf{M}} \,, \tag{2}$$

$$S_{\rm FM} = E_{\rm FM}(A_{\rm F} + A_{\rm M})$$

$$=E_{\rm F}A_{\rm F}+E_{\rm M}A_{\rm M}\,,\tag{3}$$

$$S_{\text{FMB}} = E_{\text{FMB}}(A_{\text{F}} + A_{\text{M}} + A_{\text{B}})$$

$$=E_{\rm E}A_{\rm E}+E_{\rm M}A_{\rm M}+E_{\rm B}A_{\rm B}\,,\tag{4}$$

where  $E_{\rm F}$ ,  $E_{\rm M}$ , and  $E_{\rm B}$  are the individual moduli of the component layers, and  $E_{\rm FM}$  and  $E_{\rm FMB}$  denote the composite moduli of the FM and FMB multilayers. The last step in Equations (3) and (4) follows from the rule that the stiffness constant of a parallel arrangement of springs is the sum of their individual spring constants. The situation for Figure 2(b) is covered by a similar set of equations, except that Equation (3) is replaced by

$$S_{MB} = E_{MB}(A_M + A_B)$$

$$= E_M A_M + E_B A_B.$$
(5)

Whereas the inverse slopes of the load-strain curves correspond to the various stiffness constants introduced above, it should also be noted that in the stress-strain format of Figure 3, the inverse slopes represent the corresponding moduli. As shown in **Table 1**, the moduli calculated from the two stripping sequences of Figures 2 or 3 are in satisfactory agreement, and yield the average moduli and stiffness constants listed in **Table 2**. Strikingly, the frontcoat modulus was found to be five times larger than that of the Mylar, whereas the backcoat modulus was approximately equal to that of the Mylar. Two important consequences of these findings are immediately apparent. Under simple tension, the initial stress in the frontcoat was five times

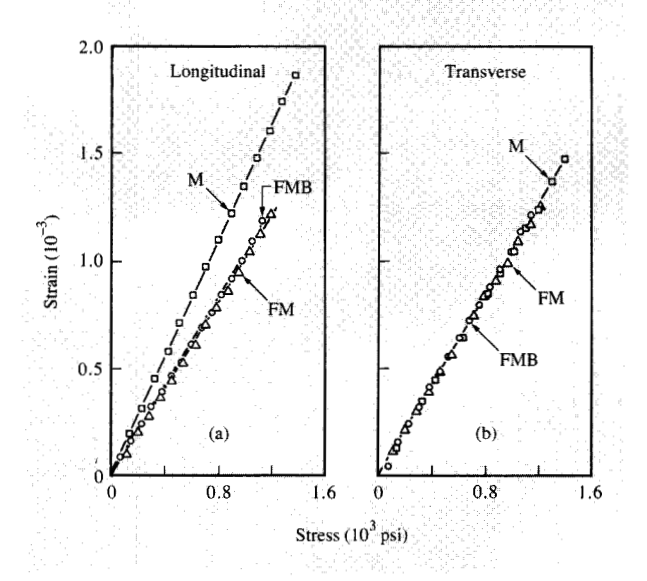
**Table 2** Young's moduli and tensile stiffness parameters of trilayer tape.

Layer		Modulus relative to Mylar	Tensile stiffness (EA) (lb)	Fractional contribution to tensile stiffness
Frontcoat	41	5.4	316	0.44
Mylar	7.6	1	348	0.48
Backcoat	7.2	0.95	58	0.08

larger than in the Mylar substrate. Secondly, despite its relative thinness, the frontcoat initially carried an impressive 44% of an applied tensile load (Table 2).

Since the frontcoat and backcoat were of nominally similar composition and thickness, the cause of their remarkably different elastic properties must be sought in terms of the different processing steps applied to each. There are two steps in the processing of the frontcoat which were omitted from the backcoat and appeared to be of possible importance. One of these two was the magnetic field orientation treatment applied to partially align the acicular CrO<sub>2</sub> particles in the liquid frontcoat media before drying. The other was the calendering (warm-rolling) treatment used to compact and secure the high surface finish on the frontcoat. To distinguish the relative importance of these two factors, we investigated a specially prepared sample for which the magnetic orientation step had been omitted. This sample, instead of being slit into tape, was supplied as 24inch-wide sheet. We were thus able to slice 1/2-inch-wide tapes from both the longitudinal and transverse directions, for the investigation of planar anisotropy in the elastic behavior. Figure 4 shows the stress-strain plots obtained with the aid of the selective stripping technique described earlier. The difference between the results for the longitudinal and transverse samples is an immediate indication of elastic anisotropy. The component moduli obtained from these plots are included in Table 3. The effect of the calendering treatment alone is evident from a comparison of the values of  $E_{\rm B}$  and  $E_{\rm E}$  listed in the last two columns. The modulus of the uncalendered backcoat was essentially isotropic, with a mean value of  $6.8 \times 10^{5}$  psi, in good agreement with that listed in Table 2. Calendering raised the transverse modulus to  $10.8 \times 10^5$  psi and, more dramatically, increased the longitudinal modulus fourfold to  $28 \times 10^{5}$  psi, thus introducing substantial anisotropy into the elasticity of the frontcoat. Although not as large as the mean value  $41 \times 10^5$  psi for oriented and calendered frontcoat, it seems clear that calendering, rather than the magnetic orientation treatment, was the principal processing step responsible for the high longitudinal stiffness of the

Finally, it is of interest to point out a remarkable coincidence in the elastic behavior reported above. As shown in Table 3, the Mylar substrate also exhibited anisotropic



#### 35,111.5

Stress-strain curves for magnetically unoriented tape, tested in the longitudinal and transverse directions. These curves indicate the dominant role of calendering in the production of a frontcoat having marked elastic directionality and high longitudinal modulus.

Table 3 Young's moduli for unoriented trilayer tape.

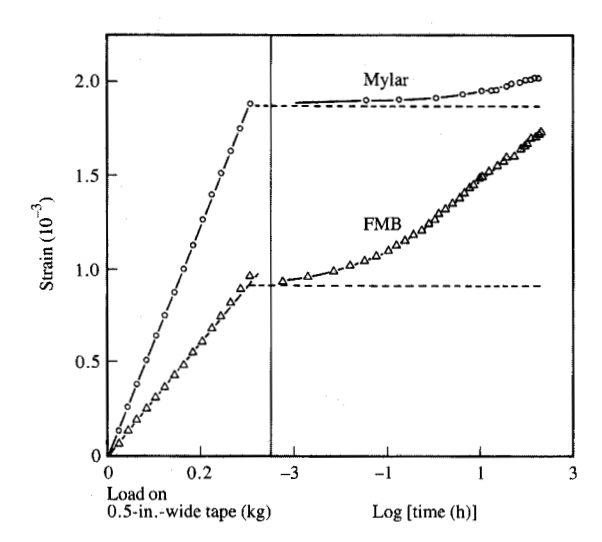
Sample orientation	$E_{ extsf{FME}}$	$E_{\rm F}$	$E_{\rm M}$	$E_{\mathtt{B}}$	$E_{ m F}$	
onemation	(10 <sup>5</sup> psi)					
Longitudinal (L)	9.5	9.9	7.3	6.6	27.8	
Transverse $(T)$	9.3	9.6	9.4	6.9	10.8	
Anisotropy ratio $(L/T)$	1.02	1.03	0.78	0.96	2.6	

behavior of lesser amount and of opposite sense to that produced in the frontcoat by calendering. When weighted by layer thickness, however, and combined to produce the composite modulus  $E_{\rm FMB}$ , these individual anisotropies largely annul each other, to produce a macroscopically isotropic trilayer with an anisotropy ratio of only 1.02 (Table 3). However, this near-isotropy must be regarded as a fortuitous characteristic of the particular samples studied, rather than as an inherent property of the trilayer tape, since it is known that the longitudinal and transverse moduli of Mylar vary with position across the width of the original roll.

## 3. Creep measurements

• Results on bare Mylar and composite tapes

Due to the viscoelastic character of both the Mylar substrate
and polymeric binder used in both the front and back



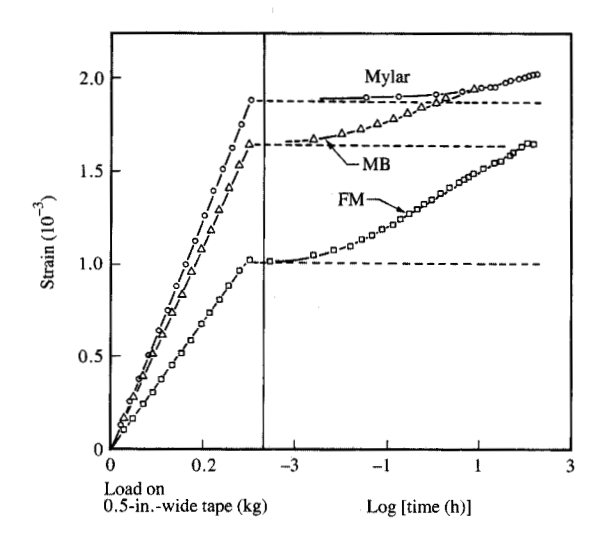


Figure 5

Isoload comparison at 295 K and 7% relative humidity of tensile creep in bare Mylar and the trilayer tape (FMB).

## Figures

Isoload comparison at 295 K and 7% relative humidity of tensile creep in bare Mylar and the bilayers FM and MB.

coatings, the imposition of a sustained tensile load produced both an initial elastic elongation and a time-dependent elongation (creep) of the tape. The amount of creep produced by service stresses is generally small (less than the initial elastic strain), and does not impair the performance of the tape, provided the distribution of the creep strain is essentially uniform in the plane of the tape. On the other hand, spatial gradients in the creep strain associated with nonuniformities in either the fabrication or loading history can lead to problems associated with warping of the tape, and for this reason a characterization of the viscoelastic response became important.

In this section, we consider the information obtainable from creep experiments performed under a constant load. It must be recognized at once that the creep of a multilayer tape represents a more complicated situation than does the creep of a single-layer tape, where (for small strains) a constant load produces a constant stress. Although a constant load imposes a constant nominal stress on the composite, the *actual* stress on each component may change substantially as the creep takes place, decreasing on the layers which relax most rapidly, and increasing on those which relax more slowly. As a consequence of the continual repartitioning of the load between the different layers, a constant load experiment on a multilayer tape represents neither creep at constant stress nor stress relaxation at constant strain.

Despite these complications, considerable insight into the viscoelastic behavior of the tape can be obtained by a

comparison of creep measurements performed on the trilayer tape and on comparison samples from which either or both of the surface coatings had been removed. In particular, we show in the next section the value of creep comparisons made on samples subject to the same constant load, a procedure we refer to as the isoload comparison method. An example of such an isoload creep comparison is shown in Figure 5 for the case of bare Mylar and the complete trilayer tape. These data were obtained with the apparatus of Figure 1. The use of a dry (≈7% relative humidity) nitrogen ambient was found to be necessary to avoid length fluctuations due to swelling and shrinkage of the tape caused by changes in atmospheric humidity. The load-strain curves obtained as a preliminary to the creep measurements are shown in the left-hand section of Figure 5; the creep subsequently observed for a period of 200 hours under a load of 0.3 kg (0.66 lb) is shown at the right. It is evident at once that the composite tape crept at a substantially higher rate than the bare Mylar, leading to a substantial relaxation of the higher stiffness initially conferred by the presence of the coatings. After 100 hours the creep strain in the composite tape was approximately eight times larger than in the bare Mylar, and after 200 hours the total strain in the composite tape was only 14% below that in the bare Mylar. To attain such a level, it is clear even without a detailed analysis that the stress in the coatings must have relaxed substantially, with a corresponding buildup in the fraction of the load carried by the Mylar substrate.

To separate the viscoelastic behavior of the front and back coatings, similar isoload comparisons were performed using tape samples from which either the front or back coatings had been removed. These results, shown in **Figure 6**, revealed at once that creep and stress-relaxation proceeded more rapidly in the backcoat than in the frontcoat. A detailed analysis of these results is presented next.

• Data analysis by the isoload comparison method
The basis of the isoload comparison technique may be explained with reference to the schematic diagrams of Figure 7. The upper section (a) shows the creep curves obtained from bare Mylar and composite tape when the same constant load was applied to each. The middle section (b) shows (via the solid lines) the constant total load L and the component loads  $L_{\rm C}(t)$  and  $L_{\rm M}(t)$  carried by the coating and Mylar of the composite tape. Unlike the creep curves shown in (a), the load-partitioning curve drawn in (b) was not known experimentally. However, since our purpose is to obtain information on the relaxation of stress in the coating,  $\sigma_{\rm C}(t)$ , we start by observing that

$$\frac{\sigma_{\rm C}(t)}{\sigma_{\rm C}(0)} = \frac{L_{\rm C}(t)}{L_{\rm C}(0)} 
= \frac{L - L_{\rm M}(t)}{L - L_{\rm M}(0)}.$$
(6)

We now wish to show that the value of  $\sigma_C(t)/\sigma_C(0)$  can be bracketed by two simple ratios obtainable from the isoload creep curves. Each of these ratios corresponds to a different limiting assumption about the form of the load-partitioning curve. Case 1 of Figure 7(b) corresponds to the assumption that throughout the interval 0 to t, the Mylar behaves elastically with a fixed modulus  $E_M^{(1)}$  given by

$$E_{\mathbf{M}}^{(1)} = (L/A_{\mathbf{M}})/\varepsilon_{\mathbf{B}}^{(1)},$$
 (7)

where  $\epsilon_{\rm B}^{(1)}$  is the initial, and by assumption, constant strain in the *bare* Mylar. The load  $L_{\rm M}^{(1)}(t)$  on the Mylar portion of the composite tape is therefore given by  $L\epsilon(t)/\epsilon_{\rm B}^{(1)}$ , and represents an upper limit on the actual load  $L_{\rm M}(t)$ . We thus can write

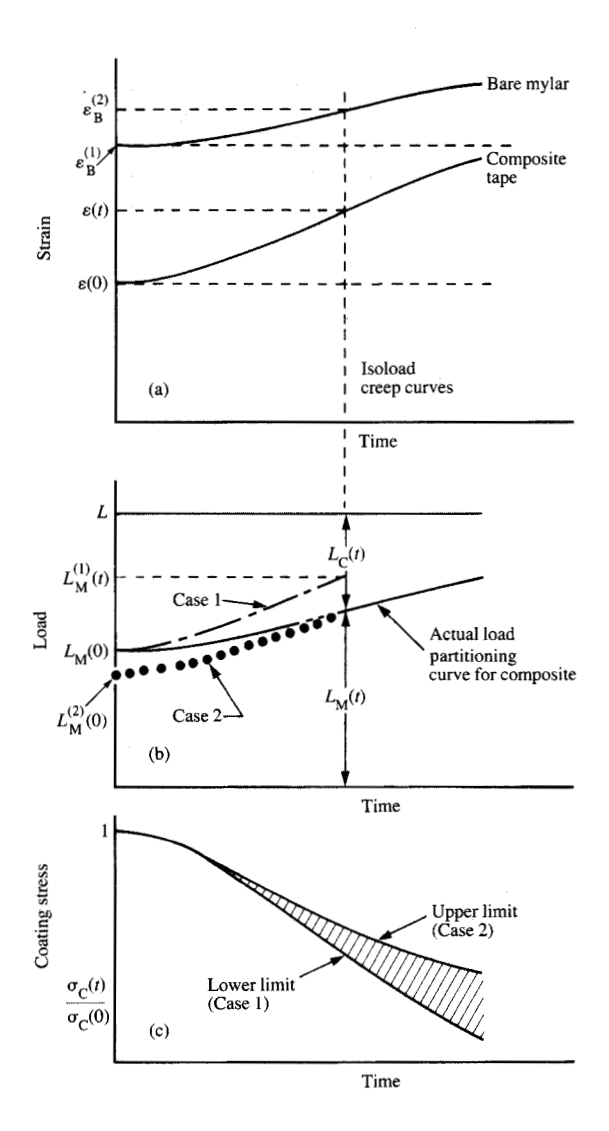
$$L_{\mathbf{M}}(t) \le L_{\mathbf{M}}^{(1)}(t) = L\varepsilon(t)/\varepsilon_{\mathbf{B}}^{(1)},\tag{8}$$

and upon insertion of Equation (8) into Equation (6), we obtain

$$\frac{\sigma_{\rm C}(t)}{\sigma_{\rm C}(0)} \ge \frac{\varepsilon_{\rm B}^{(1)} - \varepsilon(t)}{\varepsilon_{\rm p}^{(1)} - \varepsilon(0)}.$$
 (9)

At the other extreme, Case 2 of Figure 7(b) corresponds to the assumption that throughout the interval 0 to t, the Mylar always behaved elastically, with a fixed modulus given by

$$E_{\rm M}^{(2)} = (L/A_{\rm M})/\varepsilon_{\rm B}^{(2)}$$
 (10)

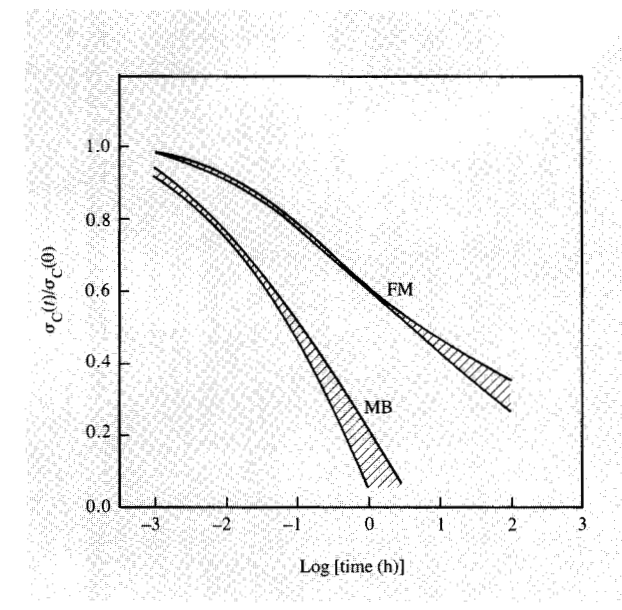


Schematic illustration of the isoload creep technique. The observed creep behavior of the bare Mylar tape and that of the coated tape are compared in (a) for the same constant load L. The lower solid line in (b) shows how the load L is actually partitioned between the Mylar and the coating in the composite tape. The precise form of this curve is unknown; however, for any time t it may be bracketed by two fictitious load histories (labeled Case 1 and Case 2) whose form may be calculated in the manner described in the text. As a consequence, it can be shown that the ratios  $[\varepsilon_B^{(2)} - \varepsilon(t)]/[\varepsilon_B^{(2)} - \varepsilon(0)]$  and  $[\varepsilon_B^{(1)} - \varepsilon(t)]/[\varepsilon_B^{(1)} - \varepsilon(0)]$  provide upper and lower limits for the normalized stress relaxation in the coating, as shown in (c).

This assumption underestimates the load history imposed on the Mylar in the composite, and leads to

(10) 
$$L_{\mathbf{M}}(t) \ge L_{\mathbf{M}}^{(2)}(t) = L_{\varepsilon}(t)/\varepsilon_{\mathbf{R}}^{(2)},$$
 (11)

687



Relaxation of the frontcoat and backcoat stresses, deduced by the isoload comparison technique. The coating stress  $\sigma_{\rm C}$  refers to the front and back coatings for the curves labeled FM and MB, respectively.

which when inserted into Equation (10) gives

$$\frac{\sigma_{\rm C}(t)}{\sigma_{\rm C}(0)} \le \frac{\varepsilon_{\rm B}^{(2)} - \varepsilon(t)}{\varepsilon_{\rm B}^{(2)} - \varepsilon(0)}.$$
 (12)

By combining Equations (9) and (12), we obtain the final result.

$$\frac{\varepsilon_{\mathbf{B}}^{(2)} - \varepsilon(t)}{\varepsilon_{\mathbf{B}}^{(2)} - \varepsilon(0)} \ge \frac{\sigma_{\mathbf{C}}(t)}{\sigma_{\mathbf{C}}(0)} \ge \frac{\varepsilon_{\mathbf{B}}^{(1)} - \varepsilon(t)}{\varepsilon_{\mathbf{B}}^{(1)} - \varepsilon(0)},\tag{13}$$

which shows how ratios formed from isoload creep data can be used to obtain the maximum and minimum limits for  $\sigma_{\rm C}(t)/\sigma_{\rm C}(0)$ . As indicated in Figure 7(c), these limits progressively diverge as relaxation occurs in the Mylar. However, as we see below, the overall spread observed in practice is not too great, because the relaxation in the Mylar is generally much smaller than in the coating. Figure 8 shows the normalized stress-relaxation curves for the front and back coatings obtained by application of Equation (13) to the creep results of Figure 6. Since the limits indicated for each curve are relatively narrow, we work with the mean values of  $\sigma_{\rm F}(t)/\sigma_{\rm F}(0)$  and  $\sigma_{\rm B}(t)/\sigma_{\rm B}(0)$  given by the centerline of each band, for the purpose of estimating the stress and load distributions in the various layers during creep of the complete trilayer tape. To this end, we observe that the total

constant load L acting on the tape can be expressed in the form

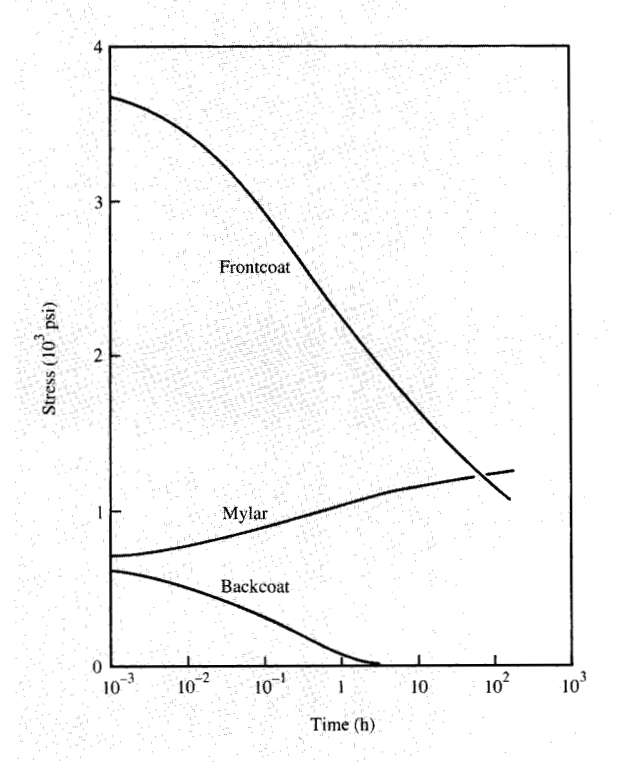
$$L_{\rm F}(t) + L_{\rm M}(t) + L_{\rm B}(t) = L_{\rm F}(0) + L_{\rm M}(0) + L_{\rm B}(0),$$
 (14)

which leads to

$$\left[\frac{\sigma_{\rm F}(t)}{\sigma_{\rm F}(0)}\right]\!E_{\rm F}^{U}A_{\rm F} + \left[\frac{\sigma_{\rm M}(t)}{\sigma_{\rm M}(0)}\right]\!E_{\rm M}^{U}A_{\rm M} + \left[\frac{\sigma_{\rm B}(t)}{\sigma_{\rm B}(0)}\right]\!E_{\rm B}^{U}A_{\rm B}$$

$$= E_{\rm F}^{U} A_{\rm F} + E_{\rm M}^{U} A_{\rm M} + E_{\rm B}^{U} A_{\rm B}. \tag{15}$$

Using Equation (15), the values of the stiffness constants EA from Table 2, and the values of  $\sigma_{\rm F}(t)/\sigma_{\rm F}(0)$  and  $\sigma_{\rm B}(t)/\sigma_{\rm B}(0)$  from Figure 8, it is then possible to calculate the stresses on the component layers, with the results shown in Figure 9. These curves serve to emphasize the high initial stress in the frontcoat, and the fact that in absolute terms the stress shed by the frontcoat exceeds by many times the maximum stress in the backcoat. Figure 9 also brings out the point that changes in the stress on the Mylar are not so great as the changes in the frontcoat, a "cushioning" effect which arises



The estimated redistribution of stress among the component layers of the trilayer tape, during creep at 295 K under a constant load of 0.66 lb.

from the greater cross-sectional area of the Mylar. It is also instructive to consider these results in terms of the repartitioning of the fractional loads carried by the different elements of the tape, as shown in Figure 10. It can be seen that initially the frontcoat and the Mylar carried almost equal loads, and that the major repartitioning involved an almost reciprocal action between these layers, with the backcoat playing a minor role.

## 4. Thermal curling measurements

In common with the bimetallic strips utilized in thermostats and other devices, a multilayer composed of materials having different expansion coefficients has a general tendency to bend or curl when subjected to a change of temperature [1]. In this section we show that thermal curling can be exploited as a useful tool for the study of recording tape. Our interest in this phenomenon arose from the observation that heat from a standard microscope illuminator (subsequently replaced by a fiber-optic illuminator) caused easily perceptible curling of the trilayer tape. We then pursued some quantitative measurements in

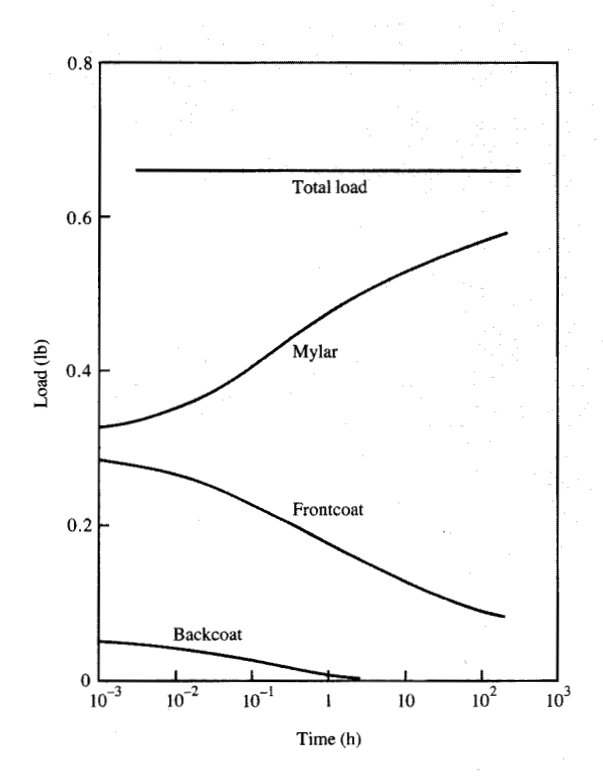


Figure 10

The estimated repartitioning of the individual loads carried by the component layers of trilayer tape, during creep at 295 K under a constant load of 0.66 lb.

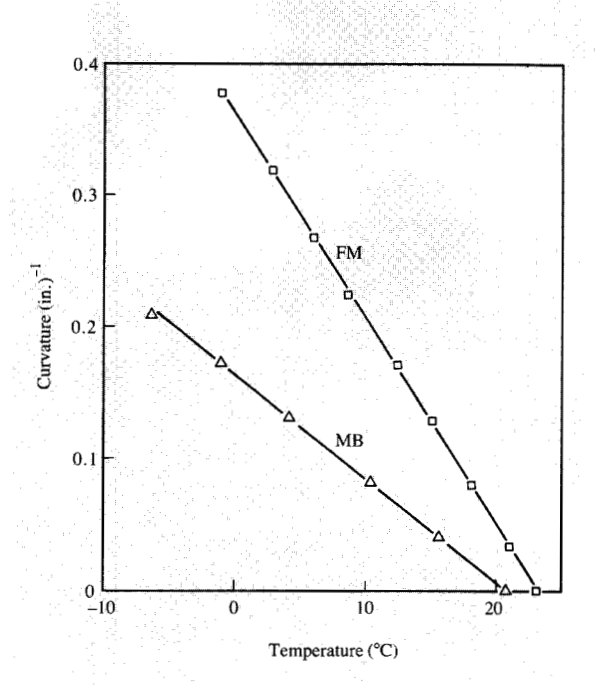


Figure 11

Thermal curling results for FM and MB bilayers.

order to understand the implications of this effect. As we shall see, it turns out that the elastic asymmetry of the trilayer is largely responsible for its thermal curling behavior, rather than a difference in the expansion coefficients of the front and back coatings.

To understand the behavior of the trilayer, we resorted once again to selective removal of the coatings to prepare FM and MB bilayer strips, cut to the dimensions  $1 \times 1/8$ inches. These samples were clamped at one end in the manner of a cantilever, and mounted on a temperaturecontrolled platform inside an environmental chamber containing dry helium. Changes in the curvature of a sample were calculated from deflection measurements made with a microscope of the type shown in Figure 1. Measurements were made on cycling below room temperature to minimize the risk of complications due to relaxation during the temperature cycle. The results of Figure 11 exhibit linear behavior with minimal hysteresis, indicating that curling occurred within the elastic regime. The sense of the curvature change is the same for both samples, and revealed at once that the Mylar had a larger expansion coefficient than the coatings. It is also evident that the slopes of the lines in Figure 11 are distinctly different, an effect which could have arisen from a difference either in the expansion coefficient or the modulus of the surface coatings. From the



#### la cintale

Samples used in the mandrel test: left, as mounted; center, wound up; right, released.

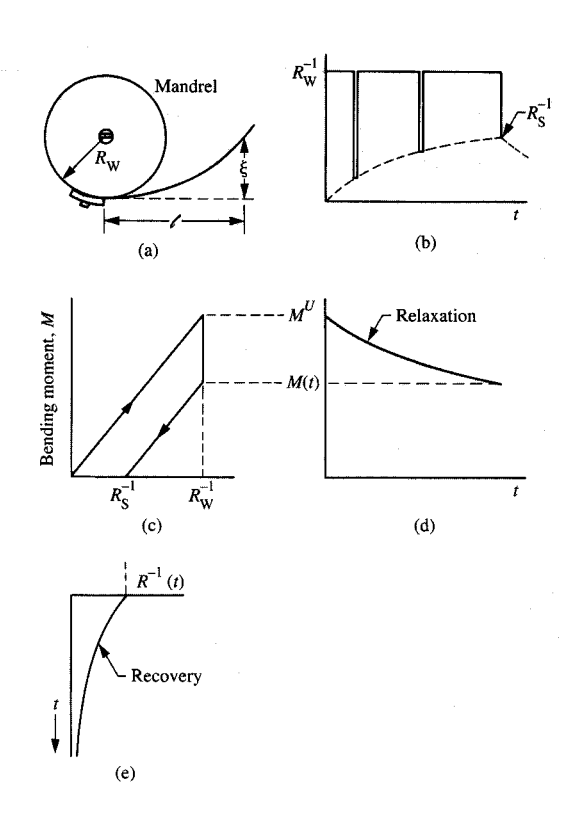


# Figure 13

Relaxation and recovery by the mandrel method: (a) geometrical layout, (b) growth of the initial spring-back curvature  $R_{\rm S}^{-1}$ , tracked by periodic momentary releases from the wound-up position, (c) moment-curvature diagram for wind-up and spring-back under unrelaxed conditions, (d) relaxation at constant curvature, and (e) recovery at zero net moment.

measured slopes, together with the component moduli given in Table 2 and the analysis in the Appendix, we obtained the differential expansion results of **Table 4**. The most striking

**Table 4** Linear expansion coefficients derived from thermal curling experiments.

Bilayer sample	Modulus ratio*	Thickness ratio	$\alpha_{\rm M} - \alpha_{\rm C}$	$\alpha_{M}$	$\alpha_{\rm C}$	
sample	$E_{\rm C}^{\rm U}/E_{\rm M}^{\rm U}$	$\alpha_{\rm C}/\alpha_{\rm M}$	(10 <sup>-6</sup> /K)			
FM	5.4	0.168	13	27 <sup>†</sup>	14	
MB	0.95	0.175	11.5	27†	15.5	

• From Table 2. The subscript C represents the coating identified by the first column.

† Average of handbook values.

aspect of these results is the close similarity of the expansion coefficients obtained for the frontcoat and the backcoat. This shows that the difference in the slopes of the FM and MB plots in Figure 11, and the thermal curling of the trilayer tape, is almost entirely accounted for by the substantial difference in the moduli of the two coatings. In contrast to the elastic modulus, it appears that the expansion coefficient of the surface coatings is not a highly structure-sensitive property. On this basis, we may expect that the magnitude of the expansion coefficient of the coatings should be determined essentially by a volumetrically weighted average of the expansion coefficients of the magnetic oxide and the polymeric binder, and in this light the results of Table 4 appear entirely reasonable.

# 5. Flexural relaxation measurements

# • The mandrel method

Early in this work, we encountered a need for a test of viscoelastic behavior that could be conveniently applied to a large number of samples. To this end, we developed the mandrel test described below for relaxation and recovery measurements on strips of tape approximately 1 inch long and 1/8 inch wide, exercised in a flexural (bending) mode of deformation. Each strip is mounted in a simple fixture consisting of a cylindrical mandrel screwed to a square reference base (Figure 12). When desired, such a fixture can be conveniently and accurately located on the stage of a microscope for measurement of the deflection  $\xi$  at a known distance  $\ell$  from the clamped end of the strip [Figure 13(a)]. The curvature of the strip 1/R may then be found from the expression

$$1/R = 2\xi/(\xi^2 + \ell^2). \tag{16}$$

In the first, or relaxation, phase of the mandrel test, the sample is wound around the mandrel and secured with a spring clip, to maintain a fixed curvature  $1/R_{\rm w}$  [Figure 13(b)]. To obtain surface strains comparable to those employed in the tension tests of Sections 2 and 3, we employed mandrels of either 3/8 in. or 1/2 in. radius. Following wind-up, viscoelastic behavior leads to a relaxation with time t of the bending moment M(t) or

bending stiffness  $K(t) = M(t)/(1/R_{\rm w})$ , as illustrated in Figures 13(c) and 13(d). Since the initial wind-up is presumed to take place rapidly under unrelaxed conditions, the slope of the wind-up line in Figure 13(c) corresponds to the unrelaxed bending stiffness  $K^U$ . To obtain the normalized relaxation function  $K(t)/K^U$ , we may, with only minor disturbance of the ideal constant-curvature condition, periodically and momentarily release the sample from the wound-up configuration, for observation of the initial spring-back curvature  $R_{\rm s}^{-1}$  [Figure 13(b)]. Since spring-back also occurs under unrelaxed conditions, it is evident that both the wind-up and spring-back lines of Figure 13(c) are parallel. From similar triangles, we thus find

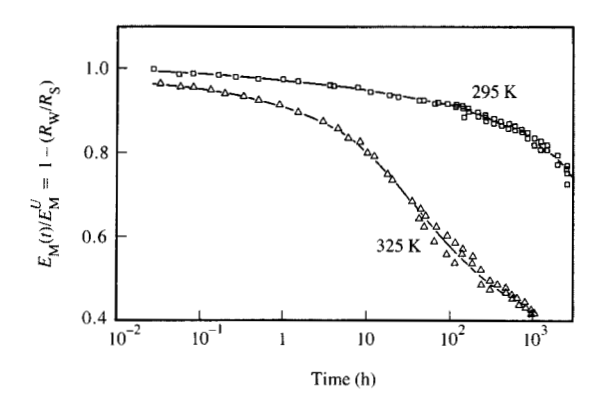
$$K(t)/K^{U} = M(t)/M^{U} = 1 - (R_{w}/R_{s}).$$
 (17)

If desired, the relaxation phase of the mandrel test may be followed by a second phase, in which the curvature exhibited upon final release is monitored for signs of recovery [Figure 13(e)]. Here, various responses may be encountered, ranging from a complete lack of recovery (viscoplastic behavior) to an eventual complete recovery (anelastic behavior).

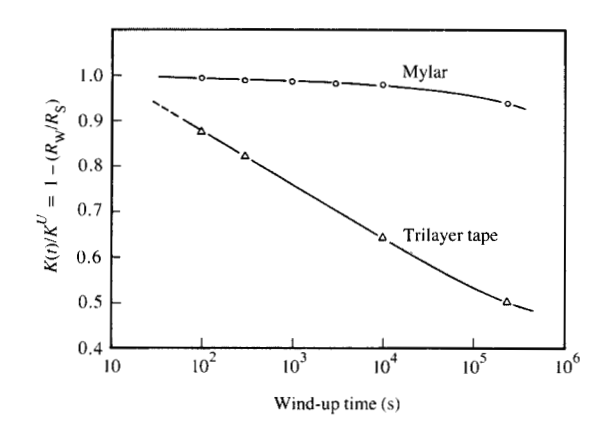
A considerable advantage of the mandrel method is the ease with which it can be employed to investigate relaxation (or recovery) behavior at elevated temperatures. The sample may be wound up, placed in a preheated oven to relax for a selected period, cooled to room temperature on a chill-block, and then released for measurement of the spring-back curvature. A detailed analysis shows that this procedure can be rigorously justified only for samples that do not exhibit thermal curling. However, the correction for a multilayer tape can be estimated from the current thermal curling response. For the tape discussed here, the correction was found to be less than 10% of the normalized relaxation stiffness  $K(t)/K^U$ , provided this ratio was greater than 0.5.

#### Illustrative results

We consider first results for bare Mylar, as an example of the application of the mandrel method to a single or unilayer test sample. For this situation, we have the considerable simplification that the neutral surface of bending remains in a constant position at the center of the strip. As a consequence, the normalized relaxation function  $K(t)/K^{U}$  in Equation (17) reduces to the normalized relaxation modulus  $E_{\rm M}(t)/E_{\rm M}^{\rm U}$ , where as before the subscript M denotes Mylar. The results of Figure 14 were obtained at room temperature (295 K) and at 325 K, using two groups of samples tested for periods of up to 100 days. At room temperature, relaxation was found to occur quite slowly. After 1000 hours, for example, it can be seen from Figure 14 that  $E_{\rm M}(t)/E_{\rm M}^{U}$ decreased by only 17%. By comparison, the relaxation was strongly accelerated at 325 K. The acceleration or shift factor between points of equal relaxation was not constant, but increased from a value of about 100 for 5% relaxation to about 160 for 25% relaxation. The effective activation



Stress-relaxation curves for bare Mylar tape, as determined by the mandrel method and spring-back measurements made 2 s after release. All samples were pre-annealed at 325 K for 40 h.



#### EGUICA F

Comparison of flexural relaxation curves at 295 K for bare Mylar tape and trilayer tape, as determined by the mandrel method.

energies corresponding to these shift factors were 1.26 eV and 1.41 eV, respectively. This increase follows the trend expected for a broad relaxation controlled by a spectrum of activated processes.

As a second example of the use of the mandrel method, Figure 15 shows the striking difference between the room-temperature relaxation behavior of bare Mylar and the complete trilayer tape. After three days, the relaxation function  $K(t)/K^U$  of the trilayer has decreased to 0.5,



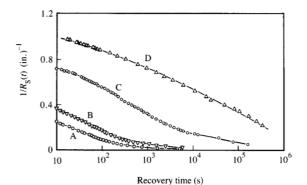


#### Figure 16

Creep recovery in the trilayer tape at 295 K after wind-up times of  $100 \, s$  (curve A),  $300 \, s$  (curve B),  $10 \, 000 \, s$  (curve C),  $235 \, 000 \, s$  (curve D). The mandrel radius was 0.5 in.

whereas the ratio for Mylar was 0.95. It is abundantly clear merely from an inspection of Figure 15 that the surface coatings exerted an overriding influence on the room-temperature relaxation behavior of the tape. A quantitative analysis of the trilayer data was complicated by a time-dependent shift in the position of the neutral surface, and is not pursued here. Nevertheless, it should be remarked that the mandrel test is inherently more sensitive to the behavior of the surface coatings than the tensile creep tests of Section 3, because bending produces the greatest strains at the surfaces of the tape.

To gain additional insight into the viscoelastic behavior of the tape, the relaxation measurements of Figure 15 were supplemented by complementary recovery experiments. For the wind-up periods employed (three days or less), the curvature developed in Figure 15 by both bare Mylar and the trilayer tape proved to be almost totally recoverable. Data for the composite tape are shown in Figure 16. The time required for recovery increased with the prior wind-up time, in the manner expected for an anelastic system governed by a wide distribution of relaxation times. It must be borne in mind, however, that the observation of recoverable behavior did not prove that the surface coatings were themselves behaving in an intrinsically anelastic (recoverable) manner. This follows from the fact that the recoverable behavior of the Mylar core would enforce pseudo-anelastic behavior on the composite tape even if the coatings themselves were totally viscoplastic. Finally, it should be noted that the recoverable behavior seen in these experiments did not continue indefinitely, but increasingly

gave way to viscoplastic behavior as the time and temperature of the deformation were increased.

# 6. Discussion

Since Mylar, which comprised approximately 75% of the cross section of the trilayer tape, is an elastically stiff material compared with the urethane binder used in the surface coatings, it seemed quite reasonable prior to this investigation to assume that the substrate would dominate the properties of the composite tape. Moreover, because of the similarity of the front and back coatings in terms of their thickness and composition, it was also tempting to speculate that the tape may represent an essentially symmetrical trilayer. From the viewpoint of analyzing the flexural viscoelastic behavior of the tape, such symmetry would represent a considerable simplification, since the neutral surface of bending would then remain fixed at its center. With this perspective in mind, perhaps the most noteworthy aspect of the present work is the radically different picture which has been revealed. The tape has emerged as a markedly asymmetrical trilayer in which the surface coatings exert a major effect on both the initial stiffness and subsequent relaxation behavior of the tape. The most significant finding was the unexpectedly high initial modulus of the oriented and calendered frontcoat, which caused the magnetically active frontcoat to be by far the most severely stressed component of the tape. Since the initial moduli of the coatings far exceeded that of the binder alone, it is clear that magnetic coatings must be treated as composite structures whose elastic behavior reflects a substantial degree of rigid-particle reinforcement. As discussed for example by Nielsen [2], the modulus of composite polymers containing rigid fillers depends on many factors, notably the volume fraction of the filler, its geometrical arrangement, the degree of adhesion to the binder, and the extent of the porosity that also may be present as a third component of the structure. The marked difference in the elastic properties of the frontcoat and backcoat can be attributed principally to the effects of the magnetic orientation and calendering treatments on these factors.

In contrast to the important role of the oxide in promoting the high initial modulus of the coatings, the viscoelastic nature of the binder has emerged as the dominant factor in the relaxation susceptibility of the tape. Although changes in the formulation of the binder can be expected to influence the kinetics of relaxation, it is also apparent from the difference in the creep behavior of the FM and MB bilayers that processing and microstructural variables also play a significant role.

Finally, we wish to point out that while the results described in this paper were obtained with simple apparatus, the methods employed nevertheless contain a variety of new features. We refer in particular to the isoload comparison technique for the analysis of tensile creep data, to the



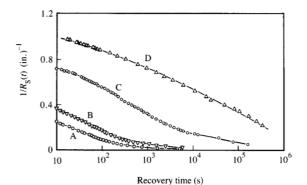


#### Figure 16

Creep recovery in the trilayer tape at 295 K after wind-up times of  $100 \, s$  (curve A),  $300 \, s$  (curve B),  $10 \, 000 \, s$  (curve C),  $235 \, 000 \, s$  (curve D). The mandrel radius was 0.5 in.

whereas the ratio for Mylar was 0.95. It is abundantly clear merely from an inspection of Figure 15 that the surface coatings exerted an overriding influence on the room-temperature relaxation behavior of the tape. A quantitative analysis of the trilayer data was complicated by a time-dependent shift in the position of the neutral surface, and is not pursued here. Nevertheless, it should be remarked that the mandrel test is inherently more sensitive to the behavior of the surface coatings than the tensile creep tests of Section 3, because bending produces the greatest strains at the surfaces of the tape.

To gain additional insight into the viscoelastic behavior of the tape, the relaxation measurements of Figure 15 were supplemented by complementary recovery experiments. For the wind-up periods employed (three days or less), the curvature developed in Figure 15 by both bare Mylar and the trilayer tape proved to be almost totally recoverable. Data for the composite tape are shown in Figure 16. The time required for recovery increased with the prior wind-up time, in the manner expected for an anelastic system governed by a wide distribution of relaxation times. It must be borne in mind, however, that the observation of recoverable behavior did not prove that the surface coatings were themselves behaving in an intrinsically anelastic (recoverable) manner. This follows from the fact that the recoverable behavior of the Mylar core would enforce pseudo-anelastic behavior on the composite tape even if the coatings themselves were totally viscoplastic. Finally, it should be noted that the recoverable behavior seen in these experiments did not continue indefinitely, but increasingly

gave way to viscoplastic behavior as the time and temperature of the deformation were increased.

# 6. Discussion

Since Mylar, which comprised approximately 75% of the cross section of the trilayer tape, is an elastically stiff material compared with the urethane binder used in the surface coatings, it seemed quite reasonable prior to this investigation to assume that the substrate would dominate the properties of the composite tape. Moreover, because of the similarity of the front and back coatings in terms of their thickness and composition, it was also tempting to speculate that the tape may represent an essentially symmetrical trilayer. From the viewpoint of analyzing the flexural viscoelastic behavior of the tape, such symmetry would represent a considerable simplification, since the neutral surface of bending would then remain fixed at its center. With this perspective in mind, perhaps the most noteworthy aspect of the present work is the radically different picture which has been revealed. The tape has emerged as a markedly asymmetrical trilayer in which the surface coatings exert a major effect on both the initial stiffness and subsequent relaxation behavior of the tape. The most significant finding was the unexpectedly high initial modulus of the oriented and calendered frontcoat, which caused the magnetically active frontcoat to be by far the most severely stressed component of the tape. Since the initial moduli of the coatings far exceeded that of the binder alone, it is clear that magnetic coatings must be treated as composite structures whose elastic behavior reflects a substantial degree of rigid-particle reinforcement. As discussed for example by Nielsen [2], the modulus of composite polymers containing rigid fillers depends on many factors, notably the volume fraction of the filler, its geometrical arrangement, the degree of adhesion to the binder, and the extent of the porosity that also may be present as a third component of the structure. The marked difference in the elastic properties of the frontcoat and backcoat can be attributed principally to the effects of the magnetic orientation and calendering treatments on these factors.

In contrast to the important role of the oxide in promoting the high initial modulus of the coatings, the viscoelastic nature of the binder has emerged as the dominant factor in the relaxation susceptibility of the tape. Although changes in the formulation of the binder can be expected to influence the kinetics of relaxation, it is also apparent from the difference in the creep behavior of the FM and MB bilayers that processing and microstructural variables also play a significant role.

Finally, we wish to point out that while the results described in this paper were obtained with simple apparatus, the methods employed nevertheless contain a variety of new features. We refer in particular to the isoload comparison technique for the analysis of tensile creep data, to the

utilization of thermal curling as a means of investigating the asymmetry of the tape, and to the advantages of the mandrel method devised for the flexural relaxation and recovery measurements. When combined with the selective stripping procedure, these methods appear to offer considerable potential for further work in the development and characterization of magnetic recording tape.

# Appendix: Thermal curling of a trilayer

The calculation of the thermal curling of a multilayer containing more than two elastic components can be handled by the same approach as that used for the bilayer [1]. However, the expressions involved rapidly become more cumbersome, and we limit the present treatment to the trilayer configuration. We denote the layer thickness by a (i = 1, 2, 3), the respective Young's moduli by  $E_i$ , and the coefficients of linear thermal expansion by  $\alpha_i$ . The trilayer is assumed to be flat and stress-free at a reference temperature  $T_0$  and to curl to a curvature 1/R in response to a temperature change  $\Delta T = T - T_0$ . The conditions for equilibrium involve (i) a balance of internal axial forces, (ii) a balance of internal bending moments, and (iii) dimensional matching at the interfaces. If we assume, following Figure 17, that the forces  $P_1$  and  $P_2$  are compressive, and  $P_3$  is tensile, the force balance may be written

$$P_1 + P_2 = P_3 \,, \tag{A1}$$

and the moment balance follows as

$$\sum M_i = \frac{P_1 a_{12}}{2} + \frac{(P_1 + P_2) a_{23}}{2}, \tag{A2}$$

where we employ the shorthand notation  $a_{ij} \equiv a_i + a_j$ . With the usual assumption that plane cross sections remain plane on bending, the bending moment on the *i*th layer is  $M_i = E_i I_i / R$ . We thus obtain

$$\frac{1}{R} \sum E_i I_i = \frac{P_1 a_{12}}{2} + \frac{(P_1 + P_2) a_{23}}{2}, \tag{A3}$$

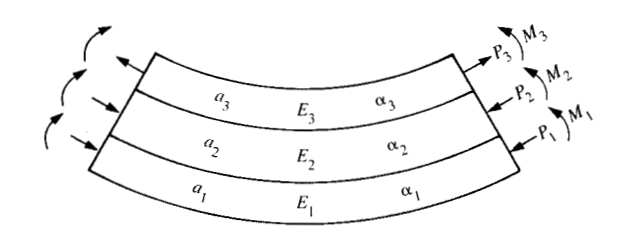
where  $I_i = ba_i^3/12$  is the second moment of area of layer i about its center, and b is the width of the cross section. Further, recognizing that the radius R is much greater than the thickness of the component layers, the requirement of dimensional matching at the interfaces leads to the equations

$$\alpha_1 \Delta T - \frac{P_1}{E_1 A_1} - \frac{a_1}{2R} = \alpha_2 \Delta T - \frac{P_2}{E_2 A_2} + \frac{a_2}{2R}$$
 (A4)

and

$$\alpha_2 \Delta T - \frac{P_2}{E_2 A_2} - \frac{a_2}{2R} = \alpha_3 \Delta T - \frac{P_3}{E_3 A_3} + \frac{a_3}{2R},$$
 (A5)

where  $A_i$  denotes the cross-sectional area  $ba_i$  of the ith layer. After elimination of  $P_3$  from Equation (A5) by the use of



# ELETTE F

Force and moment diagram for thermal curling of a trilayer.

Equation (A1), rearrangement of Equations (A4) and (A5) vields

$$X_{12} = \frac{P_1}{S_1} - \frac{P_2}{S_2},\tag{A6}$$

$$X_{23} = \frac{P_1}{S_2} + P_2 \frac{1}{S_2} + \frac{1}{S_2}, \tag{A7}$$

where the tensile stiffnesses  $S_i$  are defined by  $S_i = E_i A_i$  and

(A1) 
$$X_{12} \equiv (\alpha_1 - \alpha_2)\Delta T - a_{12}/2R$$
 (A8)

and

$$X_{23} = (\alpha_2 - \alpha_3)\Delta T - a_{23}/2R.$$
 (A9)

Solving Equations (A6) and (A7) for  $P_1$  and  $P_2$ , we obtain

$$P_1 = \frac{S_1 \{ (S_2 + S_3) X_{12} + S_3 X_{23} \}}{\sum S_i}$$
 (A10)

and

(A3) 
$$P_2 = \frac{S_2 \{ S_3 S_{23} - S_1 X_{12} \}}{\sum S_i}$$
 (A11)

When these results are inserted into Equation (A3), we finally obtain

$$\frac{1}{R} \left\{ [2(\sum S_i)(\sum E_i I_i)] + \frac{S_1 S_{23} a_{12}^2}{2} + [S_1 S_3 a_{12} a_{23}] + \frac{S_3 S_{12} a_{23}^2}{2} \right\}$$

$$= (\alpha_1 - \alpha_2) \Delta T S_1 (a_{12} S_{23} + a_{23} S_3)$$

$$+ (\alpha_2 - \alpha_3) \Delta T S_3 (a_{12} S_1 + a_{23} S_{12}). \tag{A12}$$

It is also of interest to examine Equation (A12) for some simpler cases. For the case of the totally symmetrical trilayer, we have  $\alpha_1 = \alpha_3$ ,  $E_1 = E_3$ ,  $S_1 = S_3$ , and  $a_1 = a_3$ . For this case

693

we obtain 1/R = 0, meaning that a symmetrical trilayer does not exhibit thermal curling, as is already evident from the postulated symmetry. For the geometrically symmetrical but elastically asymmetrical trilayer which approximately represents the present tape, Equation (A12) shows only a modest simplification. The case of the bilayer is obtained by assigning any one of the layers  $a_i$  a zero thickness. For example, if  $a_3 = 0$ , Equation (A12) becomes

$$\frac{1}{R} \left[ \left( \frac{2}{a_{12}} \right) \left( \frac{1}{S_1} + \frac{1}{S_2} \right) (E_1 I_1 + E_2 I_2) + \frac{a_{12}}{2} \right] 
= (\alpha_1 - \alpha_2) \Delta T,$$
(A13)

in accord with previously available results [1].

# **Acknowledgments**

The opportunity to become involved in work on magnetic tape was provided by D. P. Seraphim. We also acknowledge useful discussions with J. J. Gniewek, B. S. Sharma, W. F. Hahn, D. Connolly, B. Bhushnan, R. Bradshaw, E. A. Bartkus, and R. F. Martin of the IBM General Products Division in Tucson, Arizona. Background information on some of the tapes used in this work was supplied to us by J. R. Koch of the Materials Analysis Group at the Tucson facility.

# References

- S. P. Timoshenko, Collected Papers, McGraw-Hill Book Co., Inc., New York, 1953, pp. 403–410.
- L. E. Nielson, Mechanical Properties of Polymers and Composites, Marcel Dekker Inc., New York, 1974, Vol. 2, Chs. 7 and 8

Received January 15, 1988; accepted for publication June 6, 1988

Brian S. Berry IBM Research Division, T. J. Watson Research Center, P.O. Box 218, Yorktown Heights, New York 10598. Dr. Berry is a Research Staff Member in the Physical Sciences Department and manager of the defects-in-solids group. His principal research interests lie in the application of mechanical relaxation techniques to the study of materials. Dr. Berry joined IBM in 1958, having previously held positions at the Fulmer Research Institute and Yale University. He received a B.Sc. degree with first-class honors from the University of Manchester, England, in 1949, and staved on to teach and to obtain an M.Sc. in 1951 and a Ph.D. in 1954. He received the Cort Research Medal from the University in the following year. He is a Fellow of the American Physical Society and is co-author (with A. S. Nowick) of the book Anelastic Relaxation in Crystalline Solids. Dr. Berry is the recipient of two IBM Outstanding Contribution Awards and one Outstanding Innovation Award.

Walter C. Pritchet IBM Research Division, T. J. Watson Research Center, P.O. Box 218, Yorktown Heights, New York 10598. Mr. Pritchet is a Senior Associate Engineer in the Physical Sciences Department, working on the application of mechanical relaxation phenomena to the study of defects in thin-layer materials. He joined IBM in 1963 and was initially involved in ultrahigh vacuum techniques and stresses in thin films. He attended the RCA Institute and received a B.S. in electrical engineering from the University of Bridgeport, Connecticut, in 1969. In 1976 Mr. Pritchet received an IBM Outstanding Innovation Award for work on amorphous ferromagnetic alloys, and in 1981 a Research Division Award for his contributions to the understanding of moisture in polymers.